SEXTUPOLE BEAM-BASED ALIGNMENT FOR FCC-ee

C. Goffing*[1,2], J. Keintzel[1], A.-S. Müller[2], F. Zimmermann[1]
[1]CERN, Geneva, Switzerland
[2]Karlsruhe Institute of Technology, Karlsruhe, Germany

Abstract

Designed to succeed the High-Luminosity Large Hadron Collider (HL-LHC), the Future electron-positron Circular Collider (FCC-ee) is a proposed next-generation collider focused on lepton collisions for high-energy physics experiments. Achieving ambitious design goals requires excellent control of the orbit and optics. Off-centre beam passage through the sextupoles results in additional focusing and defocusing, together with coupling due to feed-down effects. The sextupole beam-based alignment (BBA) is considered as an addendum to the quadrupole BBA because it reduces both the dipole kicks in the magnet and the optics perturbations from feed-down effects by reducing the beam offset in the sextupole. Various approaches for the individual and parallel sextupole BBA are considered and compared.

INTRODUCTION

In 2020, the European Strategy for Particle Physics Update (ESPPU) [1] identified an Electroweak and Higgs-factory as the highest priority next collider following the High Luminosity Large Hadron Collider (HL-LHC) [2]. One option is the Future electron-positron Circular Collider (FCC-ee) [3–5]. To achieve the high luminosity value of $1.44 \times 10^{36}\,\mathrm{cm}^{-2}\,\mathrm{s}^{-1}$ at 45.6 GeV [6], excellent orbit and optics control are required, and therefore, implying strict boundaries on the accelerator optics and, thus, on the alignment tolerances of all lattice elements. In particular, the transverse offsets of beam-position monitor (BPM) readings with respect to the centre of adjacent quadrupole and sextupole magnets should be below 20 µm after Beam-Based Alignment (BBA) [6, 7]. Based on the measured offset between magnet and BPM, the beam is centred in the magnets using orbit correctors reducing the effective misalignment.

Misaligned sextupoles change the optics directly through focusing and introduction of coupling. For FCC-ee, sextupoles and quadrupoles are planned to be placed side by side with orbit and optics correctors and beam position monitors (BPMs) in the arc sections, which cover about 85 % of the circumference [6, 8, 9]. Beam-based alignment for FCC-ee is planned for the quadrupoles [10–12]. Sextupole BBA [10] is a possible complementary procedure in the arc sections and a necessary step for the interaction regions. Perturbations caused by sextupole magnets for which the beam is not well centred are compensated by steering magnets along with, normal or skew quadrupole correctors for correction of tune shifts and coupling. In the following, we present an overview of the approaches studied for an individual and parallel sextupole BBA in the arcs.

* christian.goffing@cern.ch

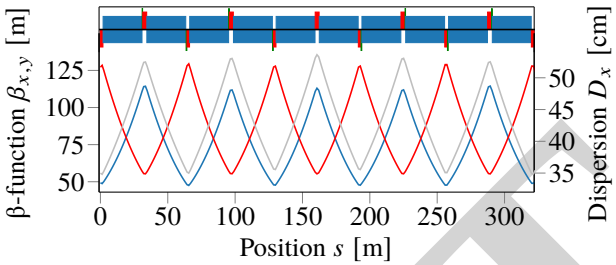

Figure 1: Shown are an LCC arc lattice cell (upper lattice diagram) as well as the horizontal (blue) and vertical (red) β-functions and dispersion D_x (grey).

Table 1: Magnet Strength and Lengths of the Different Arc Sextupole Families for LCC Lattice at Z

Sextupole family	Strength [T m^{-2}]	Length [cm]	Number of sextupoles
SD1A	−39.07	52	408
SD2A	−25.87	52	408
SF1A	46.29	30	408
SF2A	33.41	30	408

ARC LATTICES

For this paper, the Local Chromaticity Correction (LCC) lattice version 105 for Z energy is considered [13]. The lattice is based on a uniform arc layout and a hybrid focusing defocusing (HFD) lattice. Every ten quadrupole magnets, divided into 4 families, form a unit cell [9]. Next to 8 of these 10 quadrupoles a sextupole magnet is located. The arc sextupoles are divided into four families and arranged in an interleaved scheme. Two sextupoles of the SD2A family form the innermost pair, followed outwards by the SF1A and SD1A families, with the SF2A sextupoles being the last and outermost. The phase advance is 51.4° (44.7°) in the horizontal (vertical) plane between two consecutive (de)focusing quadrupoles. Each of the eight arc sections consists of 27 cells. The magnet layout and optics functions are shown in Fig. 1, and the parameters for the arc sextupoles are given in Table 1. Skew quadrupoles are planned to be integrated into the sextupoles in the form of trim windings [14–16].

SIMULATION SETTINGS

In our simulations, the BPMs and vertical orbit correctors are attached at the end of each quadrupole, close to the sextupoles. The horizontal correctors are attached to the end of the dipoles, next to the quadrupole. The nominal collision optics at Z energy is used for the simulations, although the BBA is intended to be part of the accelerator commissioning [6, 7], where a series of different optics

Table 2: Magnet Misalignment and Field Errors in Arcs and Technical Straights (TS)

Element	$\sigma_{x,y}$ [µm]	σ_θ [µrad]	σ_z [µm]	$\Delta k/k$ [10^{-4}]
Arc quads & sexts*	50	50	100	2
Girder	150	150	500	-
Arc Dipoles	1000	1000	500	10
BPM-to-quad	100	10	-	-
TS quads & sexts	50	50	100	2
TS Dipoles	1000	1000	100	10

* Misalignment relative to girder

with relaxed β^* are envisioned. Therefore, we start from a "pseudo-ballistic" model setup, where only the magnets of the arcs and the technical straights are misaligned in all three directions and rotated around the beam axis, according to the errors specified in Table 2. The σ values of the table represent one standard deviation for a Gaussian distribution truncated at 2.5 σ. The value of 10 µrad for the rotation of the BPMs around the beam axis has been identified as unfeasible and needs to be updated in the future. In the first step, misalignment and field errors are inserted for the magnets in the Xsuite [17] simulation before a closed orbit is sought using threading and orbit correction, considering 1 µm uncertainty on the closed orbit measurement. For measurements of tune or phase advance and the resonance driving term (RDT) $|\triangle f_{1001}|$, rms errors of 10^{-5} and 10^{-4} are assumed, respectively. Finally, a BPM-to-quadrupole misalignment of 100 µm rms is added.

SEXTUPOLE BBA TECHNIQUES

Misaligned sextupoles give rise to additional quadrupole and dipole field components due to feed-down. For both vertical and horizontal beam offsets, the beam is deflected in the horizontal plane. The kick strength is proportional to the squared offset. A horizontal offset causes an additional quadrupole component, whose strength depends linearly on the offset. In the vertical plane, a skew quadrupole component similarly arises. The BBA detects the presence of these additional field components, which are proportional to the offset or its square, respectively, and which linearly depending on the sextupole strength. The effects on the orbit, tune, phase advance, and f_{1001} are all possible observables. Except for the tune, the induced changes in local parameters differ for different source locations, enabling a parallel BBA.

Individual BBA Without Orbit Changes

The changes of the betatron tunes are used to reconstruct the strength of the feed-down quadrupolar component. This approach requires only variation in the sextupole strength and does not involve orbit changes. The offset between the beam and the magnetic centre is the proportionality factor between the sextupole strength, which is varied over a range from 10 % to 100 % of its nominal strength, and the reconstructed quadrupole component. Due to the moderate sextupole strength and the smallness of the relevant offsets, a high modulation amplitude is required to achieve measurable tune changes. Large β-functions at the sextupole enhance the tune changes, which has a positive effect on the accuracy of the reconstruction. The BBA is performed for all sextupoles and the simulated data and contour plots are shown in Fig. 2. As a result, this approach is rather fast and, in these simulations, yields an rms BBA error of 19.7 µm.

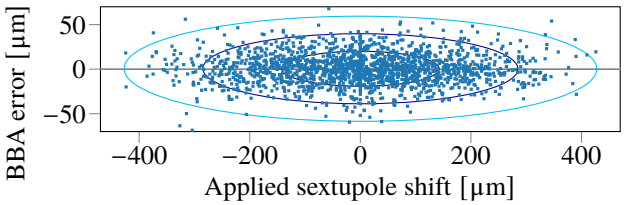

Figure 2: The dependency of the BBA error on the magnetic shift is shown here, including both the data points and the contour plots corresponding to the 1σ, 2σ and 3σ regions. The BBA reconstructs the offset based on tune changes.

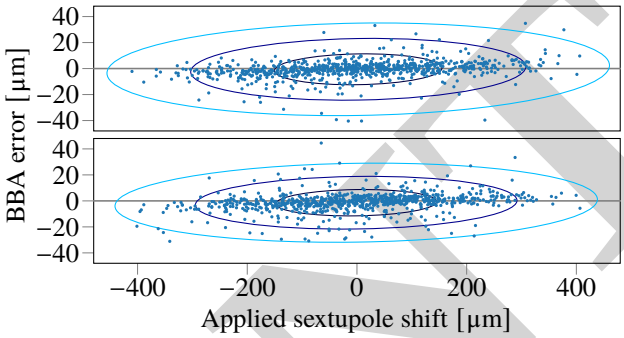

Figure 3: The figure shows the dependence of the BBA error on the sextupole shift for an individual, orbit-based BBA approach for the horizontal (top) and vertical (bottom) planes. The ellipses mark the 1σ, 2σ and 3σ regions respectively.

Individual BBA With Orbit Changes

These simulations apply a local 3-corrector bump with six different heights in the range of ±600 µm to vary the beam position at the sextupole. For each beam position, the sextupole strength is varied in the range of 25 % to 125 %

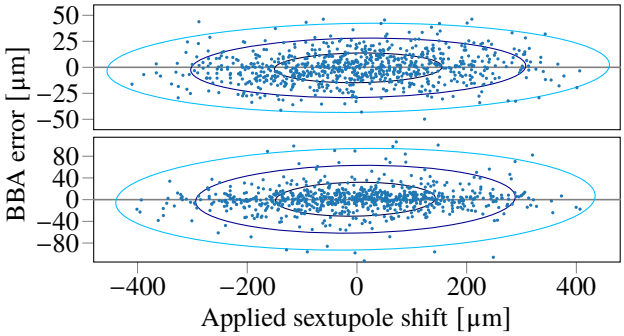

Figure 4: The figure shows the dependence of the BBA error on the sextupole shift for an individual, horizontal (top) tune- and vertical (bottom) RDT-based BBA approach. The ellipses mark the 1σ, 2σ and 3σ regions respectively.

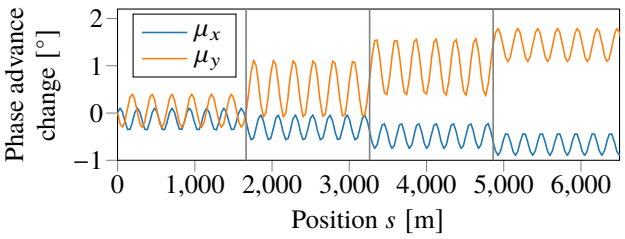

Figure 5: The figure shows the change in phase advance caused by altered quadrupole fields at the positions marked by vertical lines.

of its nominal strength and the orbit change is evaluated. When the beam passes through the centre of a sextupole, the change of tune, orbit or coupling due to the modulated sextupole strength vanishes. The results of the simulation for the orbit-based approach are shown in Fig. 3 for 812 sextupoles. Alternatively, tune and RDT variations are used for the horizontal and vertical BBA, respectively. The results are shown in Fig. 4. The orbit-based BBA is challenging, as it requires extensive averaging, given that the assumed BPM noise is comparable to the induced orbit shift caused by the sextupoles. Changing the nominal sextupole strength of a SF2A magnet between 0 % and 100 % and assuming a beam offset of 100 µm offset gives an rms orbit shift of 34 nm. The rms BBA errors are 11.9 µm and 10.2 µm for the orbit-based, and as 14.3 µm and 31.2 µm for the tune and coupling based approaches.

Parallel BBA

One can use response matrices to attribute orbit, tune or RDT f_{1001} changes to individual sextupoles, despite several of them being modulated in parallel. Due to the weak sextupoles, the signal is correspondingly small, and measurement errors affect the final result. This has already been observed for orbit-based parallel sextupole BBA [10].

The BBA simulation modulates every 10^{th} magnet of a family, 6 magnets in parallel and a modulation amplitude of 40 % for all arc sextupoles. The distance between modulated magnets is sufficient to get separated steps in the difference in phase advance caused by the feed-down quadrupole fields, as shown in Fig. 5. The results are shown in Fig. 6. From the difference in the phase advance change before and after the sextupole, the step height, the quadrupole component and, consequently, the beam offset in the sextupole are determined

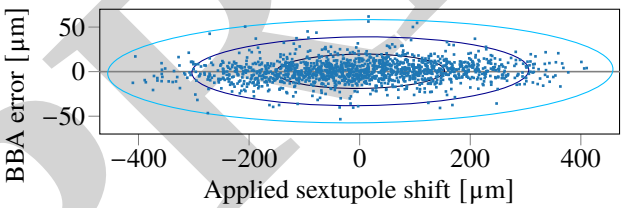

Figure 6: The figure shows the dependence of the BBA error on the sextupole shift for a parallel, phase advance-based BBA approach for the horizontal plane. The ellipses mark the 1σ, 2σ and 3σ regions respectively.

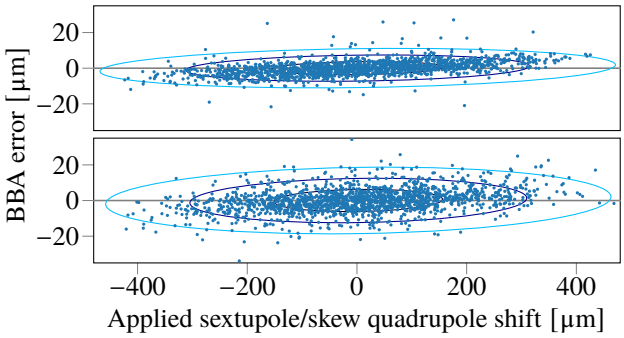

Figure 7: This figure shows the dependence of the BBA error on the sextupole/skew quadrupole shift, with the 1σ, 2σ and 3σ contour lines.

analogously to the individual tune-based BBA. The rms BBA error is 19.3 µm for a spacing of 1.6 km between modulated magnets.

PARALLEL SKEW-QUADRUPOLE BBA

As an alternative to the sextupole, the integrated trim skew quadrupole is used for the BBA. Varying the skew quadrupole strength and keeping the beam position constant by compensating the dipole kicks from the modulated magnets with the orbit correctors nearby. The offset between the beam and the magnetic centre is estimated from the changes in kick and skew quadrupole strength. A similar approach is also explored for the quadrupole BBA at FCC-ee [11, 12]. For the skew quadrupole BBA, a suitable coordinate system must be chosen, looking at the response in the plane orthogonal to the steering. The BBA results with a modulation amplitude of 1×10^{-4} m^{-1} for 51 magnets in parallel are shown in Fig. 7. Here, a more prominent rotation of the ellipses is visible. This indicates a systematic error proportional to the magnetic offset, which is attributed to the orbit slope introducing a systematic shift in the transverse beam position between the BPM and the sextupole centre.

SUMMARY AND OUTLOOK

Due to the moderate sextupole strengths, sextupole BBA presents a challenge. Individually, the accuracy appears to be below 20 µm with a tune or orbit-based approach in the horizontal plane and an orbit-based approach in the vertical plane. In the arcs, the individual and parallel sextupole BBA approaches which we have studied are not considered operationally feasible, either due to time constraints or due to a serial powering of sextupole families. Sextupole beam-based alignment using skew quadrupole trim coils has achieved sufficient accuracy to simultaneously determine the magnetic centres of 52 magnets. Further studies are needed to evaluate possible shifts in the magnetic centres of the skew quadrupole and sextupole as a function of the magnet excitation. Finally, thanks to the stronger sextupoles and larger β-functions, the sextupole BBA schemes discussed in this paper could be a promising technique for the FCC-ee interaction regions.

REFERENCES

[1] The European Strategy Group, "Deliberation document on the 2020 update of the european strategy for particle physics", CERN, Geneva, Switzerland, Rep. CERN-ESU-014, 2020. doi:10.17181/ESU2020Deliberation

[2] *High-luminosity large hadron collider (HL-LHC): technical design report*, G. Apollinari *et al.*, Eds. Geneva, Switzerland: CERN, 2020. doi:10.23731/CYRM-2020-0010

[3] M. Benedikt, A. Blondel, P. Janot, M. Mangano, and F. Zimmermann, "Future circular colliders succeeding the LHC", *Nat. Phys.*, vol. 16, no. 4, pp. 402–407, 2020. doi:10.1038/s41567-020-0856-2

[4] F. Zimmermann, M. Benedikt, K. Oide, and T. Raubenheimer, "The electron-positron future circular collider (FCC-ee)", in *Proc. NAPAC'22*, Albuquerque, NM, USA, pp. 315–320, Aug. 2022. doi:10.18429/JACoW-NAPAC2022-TUZD1

[5] M. Benedikt *et al.*, "Future circular collider feasibility study report", CERN, Geneva, Switzerland, Rep. CERN-FCC-PHYS-2025-0002, 2025. doi:10.17181/CERN.9DKX.TDH9

[6] M. Benedikt *et al.*, "Future circular collider feasibility study report volume 2: accelerators, technical infrastructure and safety", CERN, Geneva, Switzerland, Rep. CERN-FCC-ACC-2025-0004, 2025. doi:10.17181/CERN.EBAY.7W4X

[7] R. Tomás *et al.*, "Optics tuning of the FCC-ee", in *Proc. IPAC'25*, Taipei, Taiwan, pp. 282–285, Jun. 2025. doi:10.18429/JACoW-IPAC2025-MOPM009

[8] K. Oide *et al.*, "Design of beam optics for the Future Circular Collider e^+e^- collider rings", *Phys. Rev. Accel. Beams*, vol. 19, no. 11, p. 111005, 2016. doi:10.1103/PhysRevAccelBeams.19.111005

[9] P. Raimondi, S. M. Liuzzo, L. Farvacque, S. White, and M. Hofer, "Local chromatic correction optics for Future Circular Collider e^+e^-", *Phys. Rev. Accel. Beams*, vol. 28, no. 2, p. 021002, 2025. doi:10.1103/PhysRevAccelBeams.28.021002

[10] X. Huang, "Beam-based alignment simulations for the Future Circular Collider electron lattice", in *Proc. IPAC'24*, Nashville, TN, USA, pp. 308–311, May 2024. doi:10.18429/JACoW-IPAC2024-MOPG08

[11] C. Goffing *et al.*, "Beam-based alignment techniques for the FCC-ee", in *Proc. IPAC'25*, Taipei, Taiwan, pp. 571–574, Jun. 2025. doi:10.18429/JACoW-IPAC2025-MOPM109

[12] A.-S. Müller. C. Goffing J. Keintzel and F. Zimmermann, "Parallel quadrupole beam-based alignment for FCC-ee", presented at IPAC'26, Deauville, France, May 2026, paper WEP5037, this conference,

[13] CERN Optics Repository, Future Circular Collider optics repository, https://gitlab.cern.ch/acc-models/fcc/acc-models-fcc-ee

[14] J. Bauche, Magnets for FCC-ee, Nov. 2023, https://indico.cern.ch/event/1277275/contributions/5365457/attachments/2753999/4794726/2023-11-16_TE-MSC_seminar-FCC-ee_Magnets.pdf

[15] A. Vorozhtsov, Feasibility study on trim coils circuits for the main arc magnets: quadrupole and sextupole, Apr. 2026, https://indico.cern.ch/event/1675106/contributions/7041744/attachments/3257991/5816071/Trim%20Coils%20in%20QDD_SF_SD_1st%20Results.pdf

[16] K. André, S. Liuzzo, P. Raimondi, and S. White, Tuning studies status for LCC, Apr. 2026, https://indico.cern.ch/event/1667088/contributions/7021270/attachments/3250668/5801173/LCC_tuning02042026.pdf

[17] G. Iadarola *et al.*, "Xsuite: an integrated beam physics simulation framework", in *Proc. HB'23*, Geneva, Switzerland, pp. 73–80, Oct. 2023. doi:10.18429/JACoW-HB2023-TUA2I1